Braz J Phys (2012) 42:100–109
DOI 10.1007/s13538-012-0059-0

SOCIEDADE BRASILEIRA DE FÍSICA

PARTICLES AND FIELDS

Gravity with Extra Dimensions and Dark Matter Interpretation: Phenomenological Example via Miyamoto–Nagai Galaxy

Patricio Letelier · Carlos Henrique Coimbra-Araújo

Published online: 7 February 2012

Abstract Any connection between dark matter and extra dimensions is revealed by the effective energy-momentum tensor associated with the theory. In order to investigate and test such a relationship, we examine a higher-dimensional space–time endowed with a factorizable general metric with a configuration such that its density profile coincides with the Newtonian potential for disk galaxies. An appropriate solution representing stratifications of mass in the central-bulge and disk part of galaxies, e.g., the Miyamoto–Nagai ansatz, is used to solve the Einstein equations. We compute the stable rotation curves of such systems and, with no adjustable parameters, accurately recover the observational data for flat or not asymptotically flat galaxy rotation curves. We present examples of density profiles and compare them to the profile obtained from purely Newtonian potentials.

Keywords Galaxies · Miyamoto–Nagai configurations · Dark matter · Rotation curves

PACS 04.50.-h · 14.80.-j · 95.35.+d · 98.80.Jk

P. S. L. passed away on June, 9th 2011. This a posthumous publication.

P. S. Letelier
Departamento de Matemática Aplicada, Instituto de Matemática, Estatística e Computação Científica, Universidade Estadual de Campinas, Unicamp, 13083-970, Campinas, São Paulo, Brazil

C. H. Coimbra-Araújo (✉)
Universidade Federal do Paraná, Campus Palotina, RuaPioneiro, 2153, 85950-000, Palotina, Brazil
e-mail: carlos.coimbra@ufpr.br

1 Introduction

Strong observational evidence, primarily from dynamical and lensing effects of galactic disks, cluster of galaxies, and a smoothly distributed cosmological background, point to the existence of the so-called dark matter. One would expect galactic disks to be very well described by Newtonian gravitational theory, yet the accelerations of stars and gases, as estimated from Doppler velocities, are much larger than those due to the Newtonian field generated by the visible matter in those systems. This defines the plateau anomaly in the rotation curves of galaxies [1–4]. Rotation curves are the major source of information on the mass distribution in spiral galaxies. They are also important to study kinematics in and to infer the evolutionary histories of galactic systems. Historically they have offered the most basic and classic evidence of the presence of dark matter in galaxies (for an exhaustive review on rotation curves, see for instance [5]).

On the other hand, it has been verified that clusters of galaxies are composed of three main components: ∼5% in mass is the optically luminous baryonic matter in hundreds of bright galaxies, ∼15% is in the form of a bright X-ray inter-cluster gas, and the remaining ∼80% is some sort of non-baryonic "missing mass." The first evidence of such "dark matter" in clusters of galaxies was provided by Zwicky in 1937 [6], who applied the virial theorem to the Coma cluster to show that most of the matter in this cluster was dark. Other estimates of cluster masses come from gravitational lensing techniques, in both the strong and weak regimes [7, 8]. When interpreted within $4D$ general relativity (GR), the lensing effect proves anomalously strong unless one assumes the presence of dark matter in quantities and

with distribution similar to those required to explain the accelerations of stars and gas. Such techniques plus the temperature fluctuations in the cosmic background radiation have confirmed the existence of dark matter.

In [9], a thin disk constructed from a space–time endowed with extra dimensions just provided the needed extra parameters to construct, without dark matter, a configuration that mimics a generic and idealized axially symmetric galaxy. Reference [9] also obtained an important result on the gravitational lensing effects of a spherical cluster within the same space–time. These findings are directly related to the dark matter problem, i.e., to the problem posed by the anomalous rotation curves of spiral galaxies [10–13], the unexpected gravitational lensing of galaxy clusters [7, 8], and the low fraction of baryons produced during nucleosynthesis [14, 15].

In this paper, we present a straightforward procedure to extend our thin-disk model, by building an isotropic configuration that could be approached as a disk-like galaxy (examples of applications of such approach to mimic spiral galaxies are reported in [16]). While in the thin-disk model the galaxy was interpreted as a flux and counterflux of geodesic particles, we here obtain a stable configuration similar to a spiral galaxy, i.e., with a central bulge and a thick disk in a particular density profile. The artificial galaxy constructed by the thin-disk model is here replaced by a richer model and a more realistic configuration. As it is well-known, spiral galaxies comprise a non-linear geometrical structure, magnetic fields, and other complex aspects. On the other hand, dark matter has more to do with the densities, pressures and dynamical behavior of the system. Here, these aspects of the problem result from our analysis of a $4D$ isotropic configuration in a multidimensional universe. A $6D$ galaxy is constructed on the basis of arguments about the simplicity of self-gravitating objects in six dimensions (even number of space–time dimensions) presented in [9]. The resulting Einstein equations admit Miyamoto–Nagai solutions describing a family of self-gravitating configurations that can be interpreted as three-dimensional models for the distribution of mass in galaxies [16, 17].

Our presentation is organized as follows: In Section 2, the field equations are calculated from a $4D$ isotropic metric plus extra terms and a Miyamoto–Nagai ansatz is used to solve them. In Section 3, a general expression for the circular geodesics in the planar part of the configuration is derived, and we argue that it approximately represents the rotation curves. Many spiral galaxies can be constructed from our results, and in Section 4, an example is presented for a well-known galaxy (NGC 3198). The density profile from the derived rotation curves is recovered and compared with the Newtonian potential and other examples. Finally, Section 5 presents concluding remarks. The appendices present a more theoretical analysis of the model, including stability ("Appendix 1") and motion equations for a test particle in gravity with extra dimensions ("Appendix 2"). In what follows, we set $c = 1$ and $G = 1$ (and hence disconsider any variations of c or G with space, time, or number of dimensions).

2 Field Equations

Consider a generalization in which our universe has $D = 4 + n$ dimensions. For an Einstein–Hilbert gravitational action, we have that

$$S = \frac{1}{16\pi}\int \mathrm{d}^4x\mathrm{d}^n y\sqrt{-{}^{(4+n)}g}\,{}^{(4+n)}R, \tag{1}$$

which leads to the field equations

$${}^{(4+n)}G_{AB} = -8\pi\,{}^{(4+n)}T_{AB}, \tag{2}$$

where $A, B = 0, 1, \ldots, 4 + n - 1$, y are the extra dimensions and the indices $(4 + n)$ remind us that the action is multidimensional. In many theories of compactified extra dimensions, a new constant G is calculated for dimensions greater than $1 + 3$. Here we relax compactification and keep the usual value of G.

Let us first consider axial-symmetric $4D$ space–times whose metric can be written in an isotropic form in cylindrical coordinates (t, R, z, φ):

$$\mathrm{d}s^2 = \mathrm{e}^{\nu(R,z)}\mathrm{d}t^2 - \mathrm{e}^{\lambda(R,z)}(\mathrm{d}R^2 + \mathrm{d}z^2 + R^2\mathrm{d}\varphi^2). \tag{3}$$

A general relativistic formulation for the Newtonian well-known galaxy models can be written in the form of the Schwarzschild metric in isotropic coordinates [17]. In addition, to extend the formalism developed in [9], we introduce n extra dimensional coordinates. Non-exotic matter then becomes possible (including a satisfactory Huygens principle) only if n is even [9]. As an example, we therefore consider the simplest choice, $n = 2$:

$$\begin{aligned}\mathrm{d}s^2 = {}&\frac{(1-f)^2}{(1+f)^2}\mathrm{d}t^2 - (1+f)^4[\mathrm{d}R^2 + \mathrm{d}z^2 + R^2\mathrm{d}\varphi^2]\\ &- \mathrm{e}^{-k}\mathrm{d}x^2 - \mathrm{e}^{k}\mathrm{d}y^2,\end{aligned} \tag{4}$$

where $f = f(R, z)$ and $k = k(R, z)$. The field equations (2) next yield the expressions for the components

of the energy-momentum tensor. The T_t^t component is calculated as

$$T_t^t = \frac{1}{32\pi(1+f)^7}\left[16\left(f_{,RR}+f_{,zz}+\frac{f_{,R}}{R}\right)(1+f)^2 + (k_{,R}^2-k_{,z}^2)(f^3+f^2+f+1)\right]. \tag{5}$$

Here as a first approximation, we assume the density profile to coincide with the Newtonian potential in $3D$ and hence rewrite (5), with visible components only, as

$$T_t^t = \frac{1}{2\pi(1+f)^5}\left(f_{,RR}+f_{,zz}+\frac{f_{,R}}{R}\right), \tag{6}$$

and therefore with the constraint

$$k_{,R}^2 - k_{,z}^2 = 0. \tag{7}$$

This approach is convenient because it describes a quantity that can be compared to observables in real galaxies. The general solutions of (6) have the form

$$k = k_1(z-R)+k_2 \quad \text{or} \quad k = k_1(z+R)+k_2, \tag{8}$$

where k_1 and k_2 are constants, and for simplicity, we will consider $k_2 = 0$. Introducing this constraint in the energy-momentum tensor, the $4D$ part reproduces the result derived by Vogt and Letelier [17]:

$$T_R^R = \frac{1}{4\pi(1+f)^5(1-f)}\left(f f_{,zz}+\frac{f f_{,R}}{R}+2f_{,R}^2-f_{,z}^2\right), \tag{9}$$

$$T_z^z = \frac{1}{4\pi(1+f)^5(1-f)}\left(f f_{,RR}+\frac{f f_{,R}}{R}+2f_{,z}^2-f_{,R}^2\right), \tag{10}$$

$$T_z^R = T_R^z = -\frac{1}{4\pi(1+f)^5(1-f)}\left(f f_{,Rz}-3f_{,R}f_{,z}\right), \tag{11}$$

$$T_\varphi^\varphi = \frac{1}{4\pi(1+f)^5(1-f)}\left[f\left(f_{,RR}+f_{,zz}\right)-f_{,R}^2-f_{,z}^2\right]. \tag{12}$$

The extra dimensional pressure part has the form

$$T_x^x = \frac{e^{-k}}{4\pi(1+f)^5}\left(f_{,RR}+f_{,zz}+\frac{f_{,R}}{R}\right), \tag{13}$$

and

$$T_y^y = -T_x^x. \tag{14}$$

The last two equations afford an interpretation of the model as part of some universal extra dimensional theory. The energy density is given by $\rho = T_t^t$, and the stresses (pressures or tensions) along a particular direction read $P_i = -T_i^i$ when the energy-momentum tensor is diagonal. Surprisingly, the component T_t^t is proportional to the usual Laplacian of the function f in *flat* cylindrical coordinates. Note that in the Newtonian limit, when $f \ll 1$, (6) reduces to the Poisson equation

$$\nabla^2\Phi = 4\pi\rho_N, \tag{15}$$

if the function f is related to the gravitational potential Φ by

$$f = -\frac{\Phi}{2}. \tag{16}$$

In this case, $\rho \to \rho_N$ and the energy conditions excluding exotic matter from the disk are

$$\rho + \sum_i P_i > 0. \tag{17}$$

The energy-momentum tensor will be diagonal ($T_z^R = T_R^z = 0$) provided f has the form

$$f = \frac{C}{\sqrt{w(R)+g(z)}}, \tag{18}$$

where C is a constant and $w(R)$ and $g(z)$ are arbitrary functions.

Complementarily, the isotropic radial and azimuthal stresses T_R^R and T_φ^φ, respectively, will be equal only if $w(R) = R^2$. The density profile ρ can then be deduced, e.g., from the Miyamoto–Nagai solutions [16], which represent stratifications of mass in the central bulges and in the disk parts of galaxies. In this case, the simplest gravitational potential providing diagonal components is

$$\Phi(R,z) = -\frac{M}{\sqrt{R^2+(a+\sqrt{z^2+b^2})^2}}, \tag{19}$$

where a, b are positive constants.

The three-dimensional density derived from (15) is

$$\rho_N(R,z) = \frac{b^2M}{4\pi} \times \frac{aR^2+(a+3\sqrt{z^2+b^2})(a+\sqrt{z^2+b^2})^2}{[R^2+(a+\sqrt{z^2+b^2})^2]^{5/2}(z^2+b^2)^{3/2})}, \tag{20}$$

and now the function $f(R,z)$, according to (16), is

$$f(R,z) = \frac{M}{2\sqrt{R^2+(a+\sqrt{z^2+b^2})^2}}. \tag{21}$$

As we will see in next sections, the gravitational potential can only be approximated by $f(R,z)$ in the Newtonian limit. The true gravitational potential will be calculated from the circular velocity of a test particle.

3 Approximated Rotation Curves from Circular Geodesics

For given configuration, the trajectories of the particles can be derived from the geodesic equations. In view of the (radial and azimuthal) stresses, the configuration can hardly be interpreted in terms of particles moving on circular geodesics. The assumption of geodesic motion being valid for particles in a very dilute gas, such as the star gas modeling a galaxy disk, it is possible to obtain the tangential velocities of particles in the disk (i.e., the approximated planar rotation curves) from geodesic equations. Assuming $\dot{R}=0$ and $\dot{z}=0$ (the particles have no radial motion and for simplicity are confined to the $z=0$ surface), the metric (4) can be rewritten as

$$\frac{(1-f)^2}{(1+f)^2}\dot{t}^2-(1+f)^4R^2\dot{\varphi}^2-\mathrm{e}^{-k}\dot{x}^2-\mathrm{e}^{k}\dot{y}^2=1, \tag{22}$$

where $\dot{x}^A=\mathrm{d}x^A/\mathrm{d}s$, which yields

$$\dot{t}^2=\left(\frac{1+f}{1-f}\right)^2\left[1+(1+f)^4R^2\dot{\varphi}^2+\mathrm{e}^{-k}\dot{x}^2+\mathrm{e}^{k}\dot{y}^2\right]. \tag{23}$$

The Euler–Lagrange equations for the x and y coordinates lead to the following geodesic equations

$$(\mathrm{e}^{-k}\dot{x})^{\cdot}=0;\quad \mathrm{e}^{-k}\dot{x}=C_x, \tag{24}$$

$$(\mathrm{e}^{k}\dot{y})^{\cdot}=0;\quad \mathrm{e}^{k}\dot{y}=C_y, \tag{25}$$

where C_x and C_y are integration constants, which can be fixed by those calculated in [18], where a stable planar configuration was obtained.

To obtain another equation, we differentiate (23) with respect to R and use (24) and (25). It results that

$$\begin{aligned}&2f_{,R}\left[\frac{(1-f)}{(1+f)^2}+\frac{(1-f)^2}{(1+f)^3}\right]\dot{t}^2\\&+2R(1+f)^3[(1+f)+2Rf_{,R}]\dot{\varphi}^2\\&-k_{,R}(\mathrm{e}^{-k}\dot{x}^2-\mathrm{e}^{k}\dot{y}^2)=0.\end{aligned} \tag{26}$$

Equations (23) and (26) form a system with variables $\dot{\varphi}^2$ and $\dot{t}^2$. Once the system is solved, the rotation curves V_C are given by

$$V_C=\sqrt{-\frac{g_{\varphi\varphi}}{g_{tt}}}\frac{\mathrm{d}\varphi}{\mathrm{d}t}=\sqrt{-\frac{g_{\varphi\varphi}}{g_{tt}}\frac{\dot{\varphi}^2}{\dot{t}^2}}. \tag{27}$$

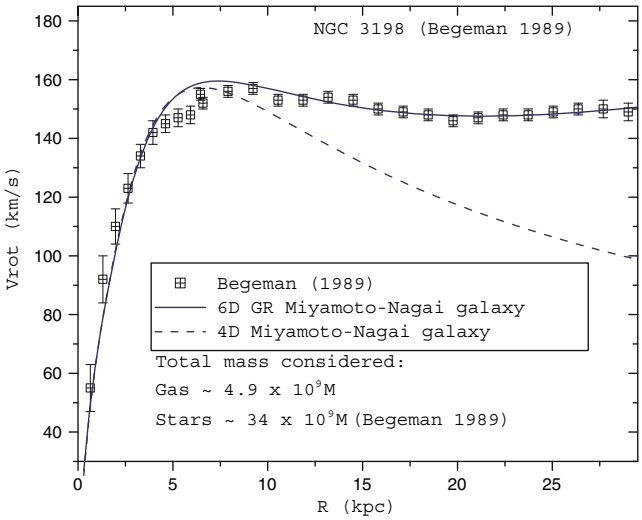

Fig. 1 Rotation curves of NGC3198 from gravitation with extra dimensions (GEDi, here with six dimensions, *solid line*) compared with a $4D$ Miyamoto–Nagai solution (*dashed line*). Only the mass of the gas and stars is included in the computation, no dark matter being considered, and the plots have no adjustable parameters. The discrepancy at 5–7 kpc is due to the gas dynamics, not accounted for in our model. The rotation curves are obtained from circular geodesics of test particles around the designed configuration. We chose $b/a=0.01$ to model a disky galaxy and the stability parameter $k_1=10^{-6}$. To enforce stability, we have also used the extra dimensional parameters $C_x=0.2$ and $C_y=0.8$

The stability of the circular geodesics is discussed in "Appendix 1."

4 Probing the Model with Real Galaxies

As shown by Miyamoto and Nagai [16], one can model a configuration like a spiral (disk-like) galaxy by adding the central and outskirt densities for different values of a and b, i.e., $\rho=\sum_i\rho(a_i,b_i)$, in other words, by a sum $\sum_i f(a_i,b_i)$ of functions f, given by (21). For a spiral galaxy, it suffices to superimpose the central bulge and the disk part.

As an example, consider the spiral galaxy NGC 3198. Given the observed disk surface density and galaxy morphology [19] and the assumption that the bulge density is similar to that of the Milky Way [16] (where a is usually set to zero and $b\sim 1\,\mathrm{kpc}$[1]), we obtain the set of stable rotation curves in Fig. 1a. Analogous results for other well-known galaxies (M31, UGC 12591, and UGC 3271) are presented in Figs. 1b, 2, and 3).

As explained in "Appendix 1", stability constrains the value of k. The parameter k_1 must be fine tuned:

[1]This means that $b/a\to\infty$, and that the central bulge is a sphere of radius $\sim$1kpc.

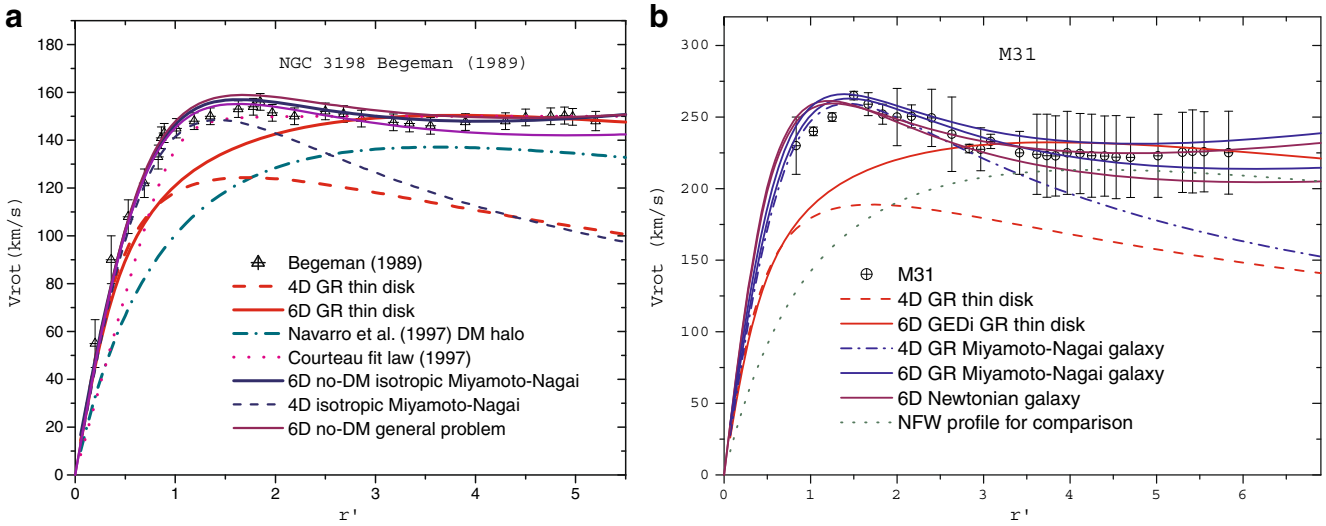

Fig. 2 Rotation velocity as a function of the radius scaled by the mass for **a** NGC3198 ($C_x = 0.2$, $C_y = 0.8$ and $k_1 = 10^{-6}$) and **b** M31 ($C_x = 0.2$, $C_y = 0.84$, and $k_1 = 3 \times 10^{-6}$)—i.e., the Andromeda Galaxy—from [19]. The data are compared with the results of various theoretical approaches: gravitation with extra dimensions, i.e., the 6D GR Miyamoto–Nagai (this work), a $6D$ GR thin disk [9] and other models [19–21]. The coordinates are the rotation velocity and the radius per mass

If $k_1 > 10^{-5}$, the rotation curves grow to infinity. By contrast, in the k_1-stable range, the rotation curves blow up moderately and coincide with many disk-like galaxy profiles. Thus, instead of adjusting k_1 to fit the experimental data, we can rely on the stability constraint to independently compute the parameter.

The gravitational potential in (19)—i.e., a Miyamoto–Nagai ansatz—is purely Newtonian and useful to calculate the form of the function f in the metric. A potential incorporating corrections from the extra dimensions can be obtained from the density by means of the equality

$$\rho = \frac{\nabla^2 \Phi}{4\pi}, \tag{28}$$

and the potential can be reconstructed from the planar circular geodesics—(27), with help of the equality

$$\Phi = \int_0^R \frac{V_C^2}{R} \mathrm{d}R, \tag{29}$$

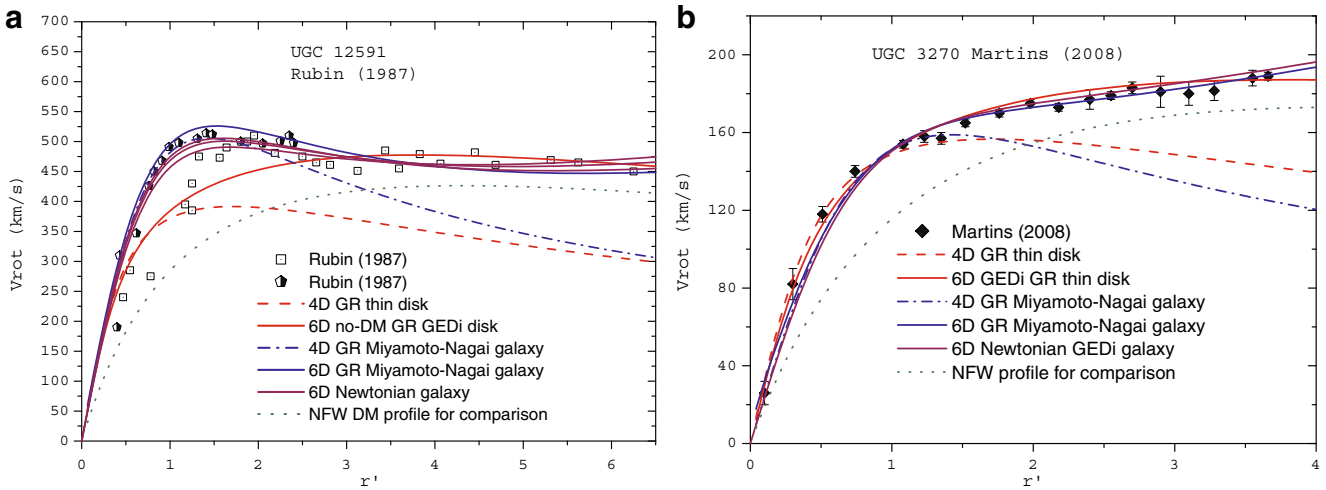

Fig. 3 Rotation curves for **a** UGC 12591 ($C_x = 0.2$, $C_y = 0.8$, and $k_1 = 3 \times 10^{-6}$) and **b** UGC 3270 ($C_x = 0.2$, $C_y = 0.85$, and $k_1 = 8 \times 10^{-6}$). Analogous to Fig. 2

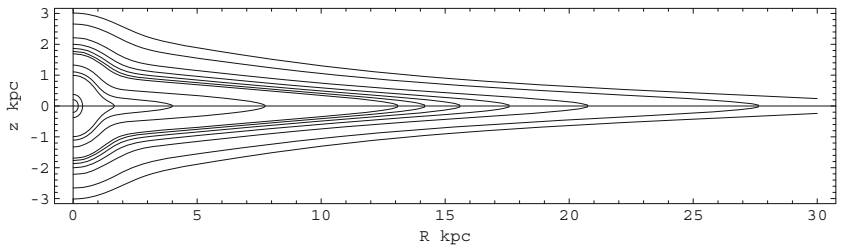

Fig. 4 The GEDi density contour plots for NGC 3198. We choose $b/a = 0.01$ to model a disk-like galaxy and the stability parameter $k_1 = 10^{-6}$. To enforce stability, we also set $C_x = 0.2$ and $C_y = 0.8$

where V_C is given by (27). The density contour plots recovered from (29) are shown in Fig. 4; our object is very similar to a spiral galaxy.

We can also compare our results with other potentials in the literature [22]. Figure 5 shows (a) the Miyamoto–Nagai potential-density pair and (b) the density recovered from our circular velocities. Another interesting reference is Satoh's potential

$$\Phi_M^{\infty}(R, z) = -\frac{M}{S}, \tag{30}$$

$$\rho_M^{\infty} = \frac{ab^2 M}{4\pi S^3(z^2+b^2)}\left[\frac{3}{a}\left(1-\frac{R^2+z^2}{S^2}\right)+\frac{1}{z^2+b^2}\right], \tag{31}$$

$$S = \left[R^2+z^2+a(a+2\sqrt{z^2+b^2})\right]^{1/2}. \tag{32}$$

Figure 6 shows various densities for the same parameters a and b. The difference between the $6D$-GR density profile and the conventional Newtonian $4D$ example is small, an indication that the extra dimensions have little effect upon the density, so that the model discussed in this paper yields the density contours in Fig. 4, very similar to real disk galaxies. By contrast, the extra dimensions have striking effect upon the shape of circular velocities.

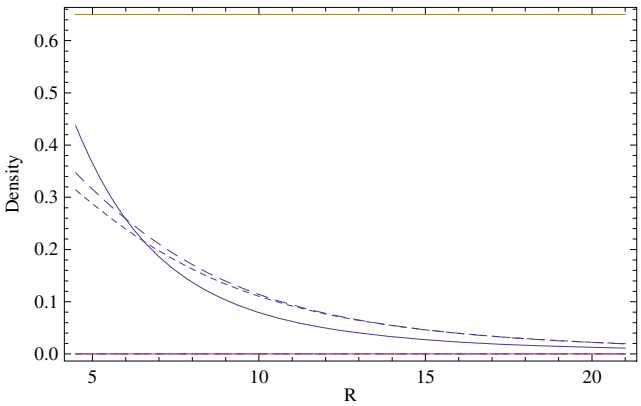

Fig. 6 Comparison between the density recovered from our circular velocities (*full line*), a pure $4D$ Miyamoto–Nagai profile (*long dash line*), and a Satoh profile (*short dash line*). Here the density, in $M_\odot/\mathrm{pc}^{-3}$, corresponds to the $3D$ configuration slice with $z = 0$ in Fig. 5. Note that beyond $R = 6$ kpc, our profile is dampened relative to the $4D$ profiles. The same damping is visible near the peak in Fig. 5b

5 Concluding Remarks

We have presented stable rotation curves for configurations in a $6D$ universe and compared our results with a few potentials in the literature. Starting out with a density profile coincident with the Newtonian potential of a perfectly symmetric configuration of a bulge plus disk, similar to a spiral galaxy, we have built a model by solving the Einstein equations with a Miyamoto–Nagai ansatz, the Miyamoto–Nagai and Satoh models offering approximate density contour plots for spiral galaxies. Phenomenology affords tests of those two potentials for the case of mass stratification in a central volume, and the contour plots of such potentials show a profile similar to what is expected for spiral galaxies.

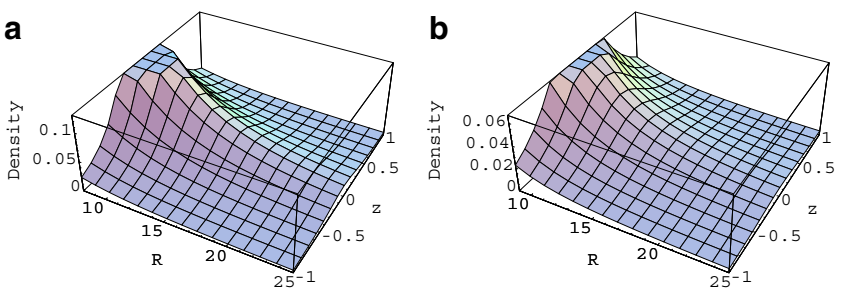

Fig. 5 **a** The Miyamoto–Nagai $4D$ model Newtonian density ρ_N, in $M_\odot/\mathrm{pc}^3$, for NGC 3198 (the non-central disk, where the rotation curve anomaly appears), as a function of R and z in kpc. **b** $3D$ plot of the recovered density profile (28) for the present model

The computed stable rotation curves for a number of galaxies reproduce the observational data with no adjustable parameters. Our semi-phenomenological approach reinforces the results in [9] and points to the conclusion that at least the rotation curves of galaxies can be explained with no reference to dark matter, provided that extra dimensions are added to the universe. As explained in [9] and also in [18], Eqs. (23)–(25) connect our model to universal extra dimensional-like theories [23], notice being taken that compactification is relaxed in our work.

The model is parametrized by the three integration constants k_1, C_x, and C_y. Our central goal being to find stable parameters with a geodesic perturbative approach, we have shown C_x and C_y to be in the range covered by the conventional thin disk calculation in [18], while k_1 is a fine-tuning stability parameter ranging from 10^{-7} to 10^{-5}. The additional parameter b/a, required by Miyamoto–Nagai configurations, must be close to 0.01 for disk-like galaxies [16].

In the solution of $k(R, z)$, one of the dimensions becomes large and the other, very small. That the important part of the galaxy rotation curve for spirals (similar to our case) occurs for $0 < R < 10R_d$, where R_d is the half-luminosity radius of the disk, is well documented [22]. Thus, with no loss of generality, in the region of interest, we set $k = k_1(z \pm R)$. As explained in Section 4 and "Appendix 1," the stability of the model is guaranteed for very small k_1, and here k_1 is in the $10^{-5} - 10^{-7}$ range for R in kpc. When $R > 10R_d$, we only have $k > 1$ for $R \sim 10^7$ kpc, a value as large as the radius of the universe. Thus, the smallness of k_1 guarantees an approximately asymptotically flat space–time in the scale of a galaxy.

Within the range of stability, our model reproduces the non-flat galaxy rotation curves. While numerous theories assuming the rotation curves of spirals to be asymptotically flat have been proposed, that assumption conflicts with observational evidence. Our model, by contrast, can explain both planar and nonplanar rotation curves. For example, parameters k_1 near the top limit of the stability bracket, i.e., $k_1 \sim 10^{-5}$, yield nonplanar curves, as Figs. 3b and 7 show.

It is not the purpose of this work to replace the dark matter paradigm, a black box that fits observations and theoretical inferences very well: not only rotation curves and lensing but also N-body numerical simulations, structure formation, and the analysis of anisotropies of the CMB. To replace this black box with another, we would have to test the latter in a wide range of theoretical and observational areas. Moreover, our phenomenological approach lies below the status of fundamental quantum field theories. Having relaxed compactification and considered only large-scale effects, i.e., phenomena at the scale of galaxy sizes, we cannot take advantage of our results to argue against the constraints of particle experiments.

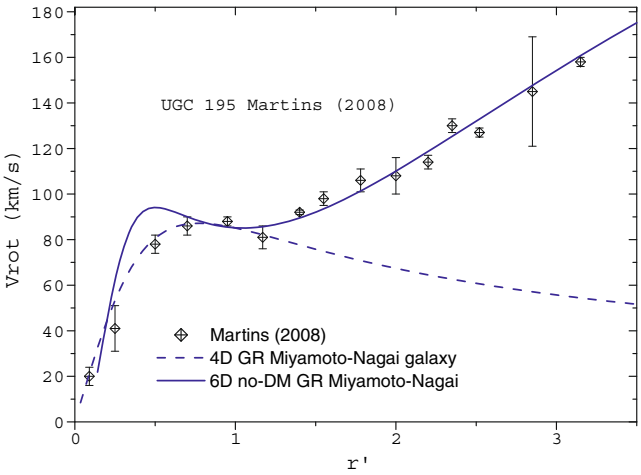

Fig. 7 The observed nonplanar rotation curve of galaxy UGC 195 [24], the Miyamoto–Nagai $4D$ expected profile and the same when it is included more two extra dimensions in computation (the case of the present model). Parameters used: $b/a = 0.01$, $C_x = 0.2$, $C_y = 0.9$, and $k_1 = 10^{-5}$

Acknowledgements The authors are very grateful to I. T. Pedron for important discussions about the main lines of the paper. The work of C.H. C. -A. is supported by PDEE/CAPES Programme under Grant No. 3874-07-9, and the work of P. S. L. was supported by the CNPq and FAPESP.

Appendix 1: Stability

For planar rotation curves, analysis of the stability is required. A general procedure has been described elsewhere [18]. Here we will study the effects of infinitesimal perturbations on the geodesic. To this end, we modify the geodesic equation $\ddot{x}^A + \Gamma^A_{BC}\dot{x}^B\dot{x}^C = 0$ with the transformation $x^A \to x^A + \Delta^A$, where $\Delta^A = (\delta t, \delta r, \delta\varphi, \delta z, \delta x, \delta y)$ are infinitesimal elements. As shown in [18], the following equations can then be derived:

$$\ddot{\Delta}^A + 2\Gamma^A_{BC}\dot{x}^B\dot{\Delta}^C + \Gamma^A_{BC,D}\Delta^D\dot{x}^B\dot{x}^C = 0, \tag{33}$$

where Γ^A_{BC} are the Christoffel symbols and $\dot{x}^A$ are proper time derivatives $\mathrm{d}x^A/\mathrm{d}s$.

For a circular orbital motion, the latter take the form

$$\dot{x}^A = (u^t, 0, 0, u^t\Omega, u^tC_x, u^tC_y), \tag{34}$$

where $\Omega = V_C/R$ (27).

Assuming oscillations in all directions with no vertical or extra dimensional restrictions, we then find that

$$\Delta^A = (\delta t, \delta R, \delta z, \delta\varphi, \delta x, \delta y). \tag{35}$$

The non-null Christoffel symbols are the following: $\Gamma^t_{tR} = \Gamma^t_{Rt}$, $\Gamma^t_{tz} = \Gamma^t_{zt}$, Γ^R_{tt}, Γ^R_{RR}, $\Gamma^R_{Rz} = \Gamma^R_{zR}$, Γ^R_{zz}, $\Gamma^R_{\varphi\varphi}$, Γ^R_{xx}, Γ^R_{yy}, Γ^z_{tt}, Γ^z_{RR}, $\Gamma^z_{Rz} = \Gamma^z_{zR}$, Γ^z_{zz}, $\Gamma^z_{\varphi\varphi}$, Γ^z_{xx}, Γ^z_{yy}, $\Gamma^\varphi_{R\varphi} = \Gamma^\varphi_{\varphi R}$, $\Gamma^\varphi_{z\varphi} = \Gamma^\varphi_{\varphi z}$, $\Gamma^x_{Rx} = \Gamma^x_{xR}$, $\Gamma^x_{zx} = \Gamma^x_{xz}$, $\Gamma^y_{Ry} = \Gamma^y_{yR}$, $\Gamma^y_{zy} = \Gamma^y_{yz}$. Let x^A be an equatorial circular geodesic in a stationary axisymmetric space–time, i.e., the worldline $x^A = (t, R = \text{const}, \varphi = \text{const} + \Omega t, z = 0, x = \text{const}, y = \text{const})$. Suppose that the solutions for δt, δR, δz, $\delta\varphi$, δx, and δy have the form of harmonic oscillations, $\sim e^{iKs}$, with a common proper angular frequency K. Substitution of the four-velocity in (34) and the non-null computed Christoffel symbols leads to the following equations for the perturbations:

$$(\ddot{\delta t}) + 2\Gamma^t_{tR}u^t(\dot{\delta R}) + 2\Gamma^t_{tz}u^t(\dot{\delta z}) = 0, \tag{36}$$

$$(\ddot{\delta R}) + 2\Gamma^R_{tt}u^t(\dot{\delta t}) + 2\Gamma^R_{\varphi\varphi}u^t\Omega(\dot{\delta\varphi}) + [(\Gamma^R_{tt,R} + \Gamma^R_{\varphi\varphi,R}\Omega^2 + \Gamma^R_{xx,R}C_x^2 + \Gamma^R_{yy,R}C_y^2)(u^t)^2]\delta R + [(\Gamma^R_{tt,z} + \Gamma^R_{\varphi\varphi,z}\Omega^2 + \Gamma^R_{xx,z}C_x^2 + \Gamma^R_{yy,z}C_y^2)(u^t)^2]\delta z = 0, \tag{37}$$

$$(\ddot{\delta z}) + 2\Gamma^z_{tt}u^t(\dot{\delta t}) + 2\Gamma^z_{\varphi\varphi}u^t\Omega(\dot{\delta\varphi}) + [(\Gamma^z_{tt,R} + \Gamma^z_{\varphi\varphi,R}\Omega^2 + \Gamma^z_{xx,R}C_x^2 + \Gamma^z_{yy,R}C_y^2)(u^t)^2]\delta R + [(\Gamma^z_{tt,z} + \Gamma^z_{\varphi\varphi,z}\Omega^2 + \Gamma^z_{xx,z}C_x^2 + \Gamma^z_{yy,z}C_y^2)(u^t)^2]\delta z = 0, \tag{38}$$

$$(\ddot{\delta\varphi}) + 2\Gamma^\varphi_{\varphi R}\Omega u^t(\dot{\delta R}) + 2\Gamma^\varphi_{\varphi z}\Omega u^t(\dot{\delta z}) = 0, \tag{39}$$

$$(\ddot{\delta x}) + 2\Gamma^x_{\varphi R}C_x u^t(\dot{\delta R}) + 2\Gamma^x_{xz}C_x u^t(\dot{\delta z}) = 0, \tag{40}$$

$$(\ddot{\delta y}) + 2\Gamma^y_{\varphi R}C_y u^t(\dot{\delta R}) + 2\Gamma^y_{yz}C_y u^t(\dot{\delta z}) = 0. \tag{41}$$

The unique real solution for this homogenous system is

$$K^2 = \frac{R_1}{3} - \frac{2^{1/3}(-R_1^2 + R_2)}{3\left[2R_1^3 - 9R_1R_2 + 27R_3 + \sqrt{4(-R_1^2+3R_2)^3 + (2R_1^3 - 9R_1R_2 + 27R_3)^2}\right]^{1/3}} + \frac{1}{3(2^{1/3})}\left[2R_1^3 - 9R_1R_2 + 27R_3 + \sqrt{4(-R_1^2+3R_2)^3 + (2R_1^3 - 9R_1R_2 + 27R_3)^2}\right]^{1/3}, \tag{42}$$

where $R_1 = (\Gamma^R_{AB,R} + \Gamma^z_{AB,z})u^Au^B$, $R_2 = (\Gamma^R_{AB,R}u^Au^B)(\Gamma^z_{AB,z}u^Au^B)$ and $R_3 = 16\Gamma^y_{yR}\Gamma^R_{yy}\Gamma^x_{xz}\Gamma^z_{xx}C_x^2C_y^2(u^t)^4$, and $\Gamma^R_{AB,R}u^Au^B = (\Gamma^R_{tt,R} + \Gamma^R_{\varphi\varphi,R}\Omega^2 + \Gamma^R_{xx,R}C_x^2 + \Gamma^R_{yy,R}C_y^2)(u^t)^2$. The system is stable if the squared epicyclic frequency $\kappa^2 = (K/u^t)^2$ is strictly positive. This occurs when the signal before the square root in (42) is positive and for $k = k_1(z + R)$ in (8).

Moreover, the stability test may play an important role in determining a stable range for the constants C_x, C_y, and k_1—the latter an integration constant due to the extra dimensions for a non-exotic system (8). The constants C_x and C_y coincide with those obtained in [18]. The constant k_1 must be very small ($k_1 \sim 10^{-5} - 10^{-7}$).

The parameters a and b (in kpc) in (21) are usually obtained phenomenologically, from the density of the galaxies[16]. Since the fraction b/a estimates how disky or spherical the galaxy is, the parameters a and b can be lumped in the new parameter b/a. Disky galaxies have $b/a \sim 0.01$. Thus, observational studies of densities and stability allow construction of a galaxy for a system modeled by gravitation with extra dimensions. All the aspects of the stability study presented above are plotted in Fig. 8.

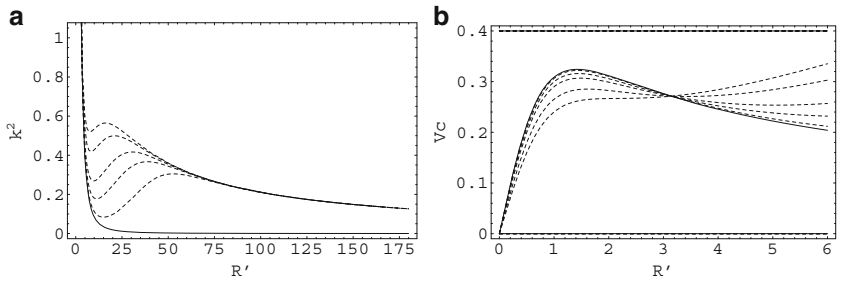

Fig. 8 **a** Stability study for the Miyamoto–Nagai configurations with extra dimensions (*dotted curves*). For comparison, the *full line* shows the $4D$ stable curve. Here $\kappa^2 = (K/u^t)^2 > 0$ represents stable curves. We have fixed $k_1 = 10^{-6}$, within the stability range, and varied C_x and C_y as indicated in Table 1. **b** Rotation curves resultant from the stable models in **a**

Table 1 Stable values for C_x, C_y, and k_1 – (8), where $k_2 = 0$

Values for k_1	Values for C_x and C_y	Region where the disk is stable
Every k_1	$C_x = 0$, $C_y = 0$ (Newtonian)	All r'
$k1 < 10^{-5}$	$0 < C_x < 0.2$, $0 < C_y < 0.4$	All r'
$k1 < 10^{-5}$	$0 < C_x < 0.2$, $C_y = 0.5$	$0 < r' \lesssim 0.4$
$k1 < 10^{-5}$	$0 < C_x < 0.2$, $C_y = 0.7$	$0 < r' \lesssim 1.4$
$k1 < 10^{-5}$	$0 < C_x < 0.2$, $C_y = 0.75$	$0 < r' \lesssim 2.6$
$k1 < 10^{-5}$	$0 < C_x < 0.2$, $C_y = 0.8$	$0 < r' \lesssim 4$
$k1 < 10^{-5}$	$0 < C_x < 0.2$, $C_y = 0.85$	$0 < r' \lesssim 5.5$ (fit DM halos)
$k1 < 10^{-5}$	$0 < C_x < 0.2$, $C_y = 0.9$	$0 < r' \lesssim 15$ (fit DM halos)
$k1 < 10^{-5}$	$0 < C_x < 0.2$, $C_y > 0.95$	Unstable disk
For values of $k_1 > 10^{-5}$	Every C_x and C_y	Unstable disk

Appendix 2: Motion Equations for a Test Particle in Gravity with Extra Dimensions

The Einstein–Hilbert gravitational action with extra dimensions is given by

$$S = \int \mathrm{d}^4x\mathrm{d}^n y\sqrt{-{}^{(4+n)}g}\,({}^{(4+n)}R + \mathcal{L}_M), \tag{43}$$

This leads to the field equations

$${}^{(4+n)}G_{AB} = {}^{(4+n)}T_{AB}, \tag{44}$$

where $A, B = 0, 1, \ldots, 4+n-1$, y are the extra dimensions and the indices $(4+n)$ describe the multidimensional nature of the action. From now, ${}^{(4+n)}G_{AB}$ and ${}^{(4+n)}T_{AB}$ will be simply called G_{AB} and T_{AB}. The same notation will describe the curvature tensor and scalar, as well as the metric.

The most general metric for the above-described space–time is

$$g_{AB}(x^\alpha) = \begin{pmatrix} g_{\alpha\beta} & | & g_{\alpha b} \\ - - - & & - - - \\ g_{a\beta} & | & g_{ab} \end{pmatrix}, \tag{45}$$

where $\alpha, \beta = (0, .., 3)$ and $a, b = (4, .., n)$, for any integer $n \geqslant 4$, and we are following the conventional treatment to turn the metric into a function of only $3+1$ coordinates. This metric, as written above, contains the explicit terms representing the $3+1$ universe and also the n terms plus crossed components. In fact, it is convenient to rewrite (45) as

$$g_{AB} = g_{\alpha\beta}\delta^\alpha_A\delta^\beta_B + g_{ab}\,\delta^a_A\delta^b_B + g_{\alpha b}\,\delta^\alpha_A\delta^b_B + g_{a\beta}\delta^a_A\delta^\beta_B, \tag{46}$$

for $A, B = (0, .., 3+n)$, where δ^i_j are the conventional Kronecker symbols.

In the particular case of a diagonal metric, we can find the derivatives and consequently the curvature terms [see Coimbra-Araújo et al. (unpublished) for the explicit calculation]. The equations of motion for such a system are calculated as

$$\ddot{x}^\mu + \left\{ {\mu \atop \alpha\beta} \right\} \dot{x}^\alpha \dot{x}^\beta = \frac{1}{2} g_{ab,\gamma} g^{\mu\gamma} N_c g^{ac} N_d g^{bd}, \tag{47}$$

where N_a denotes a vector containing, e.g., the parameters C_x and C_y (for the case of $6D$). The metric elements should be calculated by a new Poisson equation (plus boundary conditions and initial values) that arises from the new terms in Einstein equations. The Miyamoto–Nagai example in the present paper is a

particular case for such approach. For a discussion, see Coimbra-Araújo et al. (submitted for publication).

Inside the disk galaxy, the extra dimensions affect gravity by means of an effective potential calculated as

$$\Phi = \phi + C\cosh(k+\delta), \tag{48}$$

where ϕ is the potential that comes from $4D$, C, and δ are constants to be calculated and k is the function associated with extra dimensions inside the metric.

References

1. J. Oort, J Bull. Astron. Inst. Neth. **6**, 249 (1932)
2. J. Oort, J Bull. Astron. Inst. Neth. **15**, 45 (1960)
3. F. Zwicky, Helv. Phys. Acta **6**, 110 (1933)
4. Smith S, Astrophys. J. **83**, 23 (1936)
5. Y. Sofue, V. Rubin, Ann. Rev. Astr. Astrophys. **39**, 137 (2001)
6. F. Zwicky, Astrophys. J. **86**, 217 (1937)
7. B. Fort, Y. Mellier, Astron. Astrophys. Rev. **5**, 239 (1994)
8. Y. Mellier, Ann. Rev. Astron. Astrophys. **37**, 127 (1999)
9. C.H. Coimbra-Araújo, P.S. Letelier, Phys. Rev. D **76**, 043522 (2007)
10. Y. Sofue et al., Astrophys. J. **523**, 136 (1999)
11. V. Rubin, Int. Astron. Un. Symp. **117**, 66 (1987)
12. O. Garrido et al., Mon. Not. R. Astron. **349**, 225 (2004)
13. Y. Sofue et al., Pac. Astr. Soc. J. **55**, 59 (2003)
14. G. Steigman, in *Big-Bang Nucleosynthesis, Cosmological Dark Matter*, ed. by J.W.F. Valle, A. Pérez. Proceedings of the International School held 4–8 October 1993 in Valencia, Spain (World Scientific, Singapore, 1994), p. 55
15. B. Moore, Nature **370**, 629 (1994)
16. M. Miyamoto, N. Nagai, Publ. Astron. Soc. Jpn. **27**, 533 (1975)
17. D. Vogt, P.S. Letelier, Mon. Not. R. Astron. **363**, 268 (2005)
18. C.H. Coimbra-Araújo, P.S. Letelier, Class. Quantum Gravity **25**, 015001 (2008)
19. K.G. Begeman, Astron. & Astrophys. **223**, 47 (1989)
20. J.F. Navarro, C.S. Frenk, S.D.M. White, Astrophys. J. **490**, 493 (1997)
21. S. Courteau, Astron. J. **114**, 2402 (1997)
22. J. Binney, S. Tremaine, *Galactic Dynamics* (Princeton University Press, Princeton, 1987)
23. T. Appelquist, H.C. Cheng, B.A. Dobrescu, Phys. Rev. D **64**, 035002 (2001)
24. C. Frigerio Martins, *The distribution of the dark matter in galaxies as the imprint of its Nature*, Ph.D. thesis, SISSA (2008)